Ionic Liquids as Bifunctional Cosolvents Enhanced CO2 Conversion Catalysed by NADH-Dependent Formate Dehydrogenase

Zhang, Zhibo; Xu, Bao-hua; Luo, Jianquan; von Solms, Nicolas; He, Hongyan; Zhang, Yaqin; Pinelo, Manuel; Zhang, Suojiang

Published in:
Catalysts

Link to article, DOI:
10.3390/catal8080304

Publication date:
2018

Document Version
Publisher's PDF, also known as Version of record

catalysts

MDPI

Article

Ionic Liquids as Bifunctional Cosolvents Enhanced CO_2 Conversion Catalysed by NADH-Dependent Formate Dehydrogenase

Zhibo Zhang [1,2], Bao-hua Xu [2], Jianquan Luo [3], Nicolas Von Solms [1], Hongyan He [2], Yaqin Zhang [2], Manuel Pinelo [1,*] and Suojiang Zhang [2,*]

1 Department of Chemical and Biochemical Engineering, Building 229, Technical University of Denmark, 2800 Kgs. Lyngby, Denmark; zhiz@kt.dtu.dk (Z.Z.); nvs@kt.dtu.dk (N.V.S.)
2 Beijing Key Laboratory of Ionic Liquids Clean Process, Key Laboratory of Green Process and Engineering, State Key Laboratory of Multiphase Complex Systems, Institute of Process Engineering, Chinese Academy of Sciences, Beijing 100190, China; bhxu@ipe.ac.cn (B.-h.X.); hyhe@ipe.ac.cn (H.H.); zhangyq@ipe.ac.cn (Y.Z.)
3 State Key Laboratory of Biochemical Engineering, Institute of Process Engineering, Chinese Academy of Sciences, Beijing 100190, China; jqluo@ipe.ac.cn
* Correspondence: mp@kt.dtu.dk (M.P.); sjzhang@ipe.ac.cn (S.Z.); Tel.: +45-52-695821 (M.P.); +86-010-8262-7080 (S.Z.)

Received: 20 July 2018; Accepted: 26 July 2018; Published: 28 July 2018

Abstract: Efficient CO_2 conversion by formate dehydrogenase is limited by the low CO_2 concentrations that can be reached in traditional buffers. The use of ionic liquids was proposed as a manner to increase CO_2 concentration in the reaction system. It has been found, however, that the required cofactor (NADH) heavily degraded during the enzymatic reaction and that acidity was the main reason. Acidity, indeed, resulted in reduction of the conversion of CO_2 into formic acid and contributed to overestimate the amount of formic acid produced when the progression of the reaction was followed by a decrease in NADH absorbance (method **N**). Stability of NADH and the mechanism of NADH degradation was investigated by UV, NMR and by DFT calculations. It was found that by selecting neutral–basic ionic liquids and by adjusting the concentration of the ionic liquid in the buffer, the concentration of NADH can be maintained in the reaction system with little loss. Conversion of CO_2 to methanol in $BmimBF_4$ (67.1%) was more than twice as compared with the conversion attained by the enzymatic reaction in phosphate buffer (24.3%).

Keywords: ionic liquids; formate dehydrogenase; NADH degradation; CO_2 conversion

1. Introduction

Carbon dioxide (CO_2) emissions from combustion of fossil fuels and its greenhouse effect on climate change (i.e., global warming) are considered a current threat [1]. To minimize environmental problems and produce clean energy, efficient utilization of CO_2 and carbon regeneration has been the focus of a tremendous amount of research [2–5]. Recently, a strategy by which CO_2 may be converted enzymatically into valuable chemicals and fuels such as formate, formaldehyde and methanol has inspired many researchers [6,7]. Obert and Dave were the first to report a cascade reaction involving the three enzymes, formate dehydrogenase (FDH), formaldehyde dehydrogenase (FaldDH) and alcohol dehydrogenase (ADH), where the product of the first reaction serves as a substrate of downstream reaction. Reduced nicotinamide adenine dinucleotide (NADH) was used as the terminal electron donor for the enzymatic reaction [8]. However, enzymatic hydrogenation of CO_2 to formic acid (CH_2O_2), formaldehyde (CH_2O) and methanol (CH_3OH) is hampered by the low concentration of CO_2 that is available for the enzyme (formic acid dehydrogenase) in the reaction mixture. Such a low

concentration may account for the common poor conversion to formic acid and hence low conversions to formaldehyde and methanol [9].

CO_2 is highly soluble in ionic liquids (ILs) and solubility can be enhanced by adjusting the anion and substituents on the cation, for instance, by fluorinating the anion or cation components [10]. These components usually interact via electrostatic forces, van der Waals forces, hydrogen bonds and other physical effects, which can explain the high solubilities of CO_2 in ILs [11–13]. For instance, at just 50 bar of CO_2 pressure, CO_2 solubility was on the order of 50% mole fraction in [Bmim][PF_6] [14]. ILs have also been used in various enzymatic reactions involving enzymes such as lipases, celluloses, and alcohol dehydrogenases [15–17]. Zhao reported that ILs were successfully applied to lipase-catalysed enantioselective esterification reactions for enhancing the stability of lipase [18]. Zhu reported that cellulase showed a higher stability than cellobiase in aqueous 1-ethyl-3-methylimidazolium acetate media for cellulose hydrolysis [19].

It has therefore been promising to perform enzymatic conversion of CO_2 in an IL environment in order to obtain better conversion efficiency. For instance, Amado employed ILs as an alternative solvent for enzymatic conversion of CO_2 to methanol [20]. However, the conversion of CO_2 did not increase significantly compared to the result obtained with the conventional buffer. In addition, Nicole and Udo reported that the changes in concentration of ILs could cause FDH inactivation to different degrees [21]. Bahareh and Khosro reported that imidazolium based ILs had a severe inhibition effect on alcohol dehydrogenase [22]. Interestingly, however, the activity of enzyme was partially recovered with diluted ILs of less than 150 mM.

Former research has focused on the activity of dehydrogenase in ILs, but investigations on the interaction between ILs and coenzyme (NADH), which could play a key role in the conversion of CO_2, have been neglected. NADH is used not only as hydrogen donor in the reduction of CO_2 but is also employed for following the progression of the reaction and thus to quantify formate [23–25]. NADH has been reported to be unstable in dilute acid by Andersen and co-workers [26]. Incubation of N-substituted dihydropyridines in acid results in the addition of water across the 2–3 double bond to yield a 3-hydroxy-tetrahydropyridine. Alivisatos and co-workers have reported that the reaction of NADH in concentrated phosphate solutions first forms 3-hydroxy-tetrahydropyridine-tinamide which then subsequently rearranges to α-$O^{2'}$-3B-cyclo-tetrahydronicotinamide adenine dinucleotide [27]. Furthermore, the same mechanism of NADH degradation in acid has been demonstrated by Norman and co-workers [28]. Degradation of NADH in the enzymatic reaction not only reduced the conversion efficiency but also led to false results of high CO_2 conversion detected by method **N** (NADH UV absorption). Even though ILs were originally included in order to increase concentration of CO_2, degradation of NADH could counteract the positive effect and decrease the efficiency of the reaction. There is, therefore, a need to investigate the activity of NADH in ILs to understand the relationship between NADH and ILs. This will contribute to effectively conducting the enzymatic reaction and determining choice of ILs to be applied in the reaction. Additionally, UV–vis spectrophotometer is used for determination of the NADH concentration and yield of formate is calculated based on the amount of NADH consumed, which is defined as method **N** in this research. In order to find a precise method for detecting directly formate, a new detection method is thereby needed for determination of product (formate) in ILs in situations where NADH is degraded. The objective of present work was thus to find a suitable method to detect formate in the presence of ILs, and to investigate the activity of NADH in ILs to improve the efficiency of the enzymatic reaction and the potential for application of ILs for CO_2 capture.

2. Results and Discussion

2.1. Comparison between CO_2 Conversions with and without IL

Determining CO_2 conversion by monitoring decrease of UV–absorbance of NADH during reaction (due to conversion of NADH into NAD, method **N**) overestimated dramatically the actual conversion of

CO_2 provided by measuring formic acid concentrations (method **C**) (Table 1). The overestimation was much higher when the reaction was performed in buffer (~60 times) as compared to the reaction carried out in a 20/80 (*v*/*v*) $BmimBF_4$/buffer mixture (~8 times). The values of CO_2 conversion provided by the **C** method are within a typical range for such an enzymatic reaction under thermodynamic equilibrium, which generally has a low conversion rate (0.002 mM·min^{-1}) at the conditions at which the reaction was performed (FDH = 1.3 μg/mL, Tris-buffer, 37 °C) [9,29]. Liu and co-workers reported a higher conversion rate for the same reaction, however the final yield of formate was at the same level (less than 1%) [30]. The higher values of CO_2 conversion by the method **N** suggested a possible degradation of NADH during reaction, which was further investigated.

Table 1. Enzymatic Conversion of CO_2 to Formate [a].

$$CO_2 + NADH \overset{FDH\ (cat.)}{\rightleftharpoons} HCOO^- + NAD^+$$

Entry	IL (V_{IL}/V_{buffer})	NADH Conv. (%) (SD)	Yield of Formate (%) (SD)
		Method N	Method C
1	Phosphate buffer (Blank)	64.6 (±3.6)	1.1 (±0.5)
2	$BmimBF_4$ (20%)	25.4 (±3.2)	2.9 (±0.4)

[a] Reaction conditions: FDH (3 μL, 0.075 U/mL), NADH (2 μmol, 1 mM), CO_2 (1 bar), buffer (100 mM phosphate, pH = 7); 37 °C, 3 h. Standard deviation (SD).

2.2. Stability of NADH in ILs

In order to evaluate the effect of temperature on NADH degradation, aqueous mixtures of NADH with $BmimBF_4$ (5.0 equiv.) were monitored over a temperature range of 10–80 °C (Figure 1A). NADH degradation curves were obtained by in-situ UV–vis spectroscopy. A remarkable reduction of NADH was observed at temperatures higher than 40 °C, whereas such reduction was alleviated at lower temperature. At 37 °C, the kinetics approximated to a first order, with a degradation energy *Ea* of 59.5 kJ mol^{-1} (Figure S5) and a degradation rate constant of 6.2 × 10^{-3} (min^{-1}). Degradation decreased exponentially with time, with 90% loss of NADH after 4 h (Figure 1B), suggesting that the decrease of the NADH concentration in the presence of FDH was not only due to CO_2 conversion, but also due to spontaneous degradation under the reaction conditions. Degradation of NADH does not only contribute to overestimate the final CO_2 conversion, but also has a direct impact in the actual conversion of CO_2 into formic acid, as it also plays a role as a substrate in the CO_2 reduction. In order to find likely structure-performance relationships and verify whether NADH degradation occurs in a wide range of ionic liquids, degradation was evaluated in five imidazolium-based ILs, including $BmimBF_4$ (Table 2). Results showed that the stability of NADH was not only dependent on temperature, but also highly dependent on the pH value of the reaction mixture. Under neutral–basic conditions, almost no degradation of NADH was detected (entry 1). In contrast, the concentration of NADH diminished markedly at lower pH values, even under weakly acidic conditions (entry 2). Notably, under strongly acidic conditions, the absorption at 340 nm assigned to NADH disappeared coincidently with the appearance of a blue-shifted peak at 332 nm (entries 3~5 and Figure S8). Finally, when DBULat (known to be a strong basic IL) was employed rather than imidazolium-based ILs (entry 6), only traces of degradation of NADH were observed (non-statistically significant).

Table 2. Stability of NADH in aqueous ILs. [a]

Entry	IL	Residue$_{(NADH)}$ (%) (SD)	pH (SD)
1	BmimDCA	100.0 (±0.1)	7.8 (±0.20)
2	EmimOAc	12.8 (±3.1)	5.3 (±0.12)
3	EmimBF$_4$	0	2.8 (±0.18)
4	BmimBF$_4$	0	2.6 (±0.18)
5	BmimDMP	0	2.3 (±0.16)
6	DBULat	99.7 (±0.6)	9.3 (±0.14)

[a] General conditions: V_{IL}/V_{H2O}: 20%; NADH (1 mM); incubation time (3 h); temperature (37 °C); Residue$_{(NADH)}$ (%) determined by absorption at 340 nm through UV–vis spectrum. Standard deviations (SD).

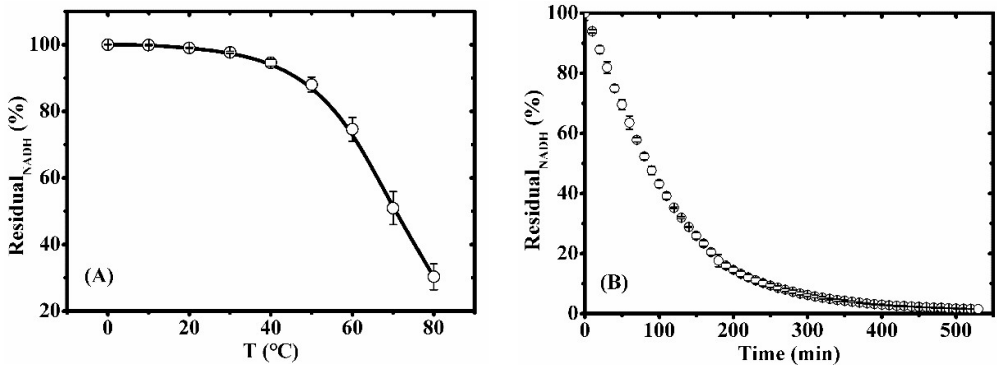

Figure 1. Study of the degradation of NADH in the presence of BmimBF$_4$. (**A**) Temperature-course plot (time interval: 10 min); (**B**) Time-course plot of degradation at 37 °C; General conditions: NADH (1.4 mg, 2 μmol); BmimBF$_4$ (2 μL, 5.0 equiv.); H_2O (2 mL).

2.3. Mechanism Discussion for NADH Degradation

2.3.1. Effect of Acidity on the Degradation of NADH

For better identification of the role of acidity on the stability of NADH during enzymatic conversion, the pH of the phosphate buffer was adjusted within the range 1.0–7.0 by the addition of proper amounts of phosphoric acid. In the absence of FDH, NADH degraded steadily with decreasing pH from 4.5 to 7.0 (Figure S6). At pH 4.5 (Figure 2), complete degradation of NADH was observed after incubation at 37 °C for 3 h. With further reduction of pH to 2.5, a new band appeared at 332 nm, and the intensity of this band gradually increased within the pH range from 2.5 to 4.5 (Figure 2). Such variation of NADH degradation with increasing acidity is consistent with our observations for the aqueous IL system in Table 2. However, the newly formed species referenced at 332 nm was not stable under extreme acid conditions, as indicated by decrease in absorbance at this wavelength over the pH range from 1.0 to 2.0.

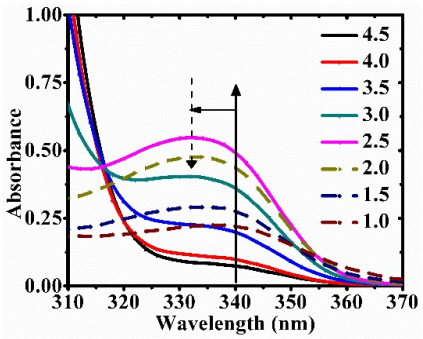

Figure 2. Degradation of NADH at pH 1.0 to 4.5. General conditions: NADH (1.4 mg, 2 μmol); phosphate buffer (2 mL); 3 h; 37 °C.

2.3.2. Proposed Mechanism of NADH Degradation

Next, a buffer solution (2 mL) of $BmimBF_4$ (V_{IL}/V_{buffer} = 20%) and NADH (2 μmol) was prepared separately for in-situ UV–vis detection at 37 °C. Initially, the presence of two typical peaks assignable to NADH at 340 and 260 nm, respectively, were observed. Upon incubation at 37 °C for 3 h, an apparent decrease of absorption intensity at 340 nm and a simultaneous increase of absorption at 260 nm were observed (Figure S7). Such variation was once referred to conversion of NADH to NAD^+ [31]. However, subsequent ^1H NMR studies indicated that a new compound besides NAD^+ was formed. Typical signals of the 1.4-dihyropyridine unit in NADH (δ: ppm), such as C(1)H_2 (2.80, 2.89), C(3)H (6.00) and C(4)H (6.95), were fully diminished (Figure 3, Figure S10, and Table S2). On the other hand, representative C-H signals of pyridinium in NAD^+ arising from hydride abstraction of NADH were not formed.

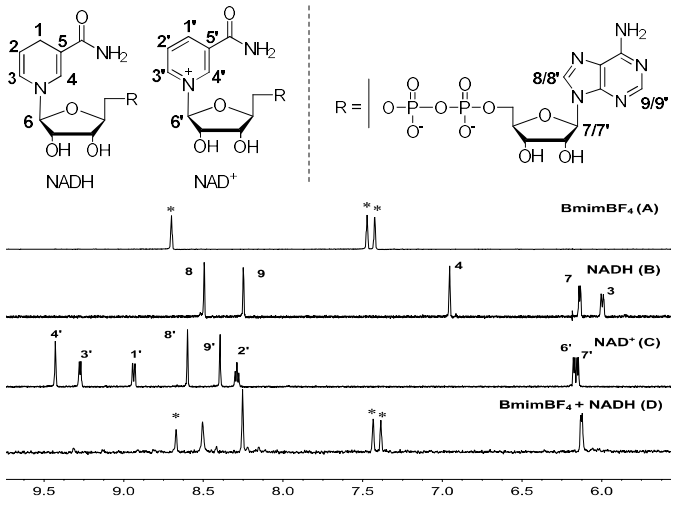

Figure 3. ^1H NMR (600 MHz, D_2O, 298 K) (δ: ppm) study. (**A**) $BmimBF_4$; (**B**) NADH; (**C**), NAD^+; (**D**) a mixture of NADH and $BmimBF_4$ (molar ratio = 1:1); * signals for imidazolium C(sp^2)-H.

DFT calculations were performed to better unravel the mechanisms of NADH degradation in acid conditions [32]. On the basis of previous literature and from our results, α-$O^{2'}$-3B-cyclo-tetrahydronicotinamide adenine dinucleotide was most likely to be the final product and two potential pathways for such conversion were evaluated (Figure S9) [28]. In pathway 1 (denoted by black curve in the Figure 4), the decomposition of NADH started with protonation of N-contained 6-membered ring at the β-position, with leading to **b**. Subsequent configuration isomerization from **b** to $\mathbf{d_1}$ occurred through ring opening of O-contained 5-memered ring. Specifically, nucleophilic addition of H_2O to the iminium cation in **b** at the α-position and C-O bond breaking of the O-contained 5-membered ring in the presence of acid affords **c**. Next, dehydrogenation of **c** at the α-position of N-contained 6-membered ring readily proceeded to generate $\mathbf{d_1}$ denoted as an α configuration, wherein the N-contained heterocycle and hydroxyl group sit at the same side of O-contained 5-memered ring (the β configuration in **b** represents two substituents sit at the opposite position). Optimization of the position of H_2O in the structure of $\mathbf{d_1}$ is found favourable in energy. A ternary hydrogen-bonding interaction system -OH/H_2O/C=O was found in the relatively stable structure **d**. Finally, the intra-molecular nucleophilic attack of OH to iminium cation of **d** affords the product **e**, coincidently with one equivalent of proton being released. In comparison to pathway 1, configuration isomerization occurred directly in pathway 2 (denoted by a red curve in the Figure 4) through an O-contained ring opening intermediate **f**. As a result, $\mathbf{d_2}$ with α configuration was formed, which is slightly different from $\mathbf{d_1}$ in pathway 1 imposed by the interaction mode towards H_2O. Subsequently, $\mathbf{d_2}$ follows the same route as $\mathbf{d_1}$ to eventually provide **e**. All structures of transitional state for both pathways are also optimized (Table S1). It suggests that the reaction leading to **d** is more likely following pathway 1 since its energy barrier step (**b**→**c**) is 3.1 kJ/mol lower as compared with that (**f**→$\mathbf{d_2}$) in pathway 2.

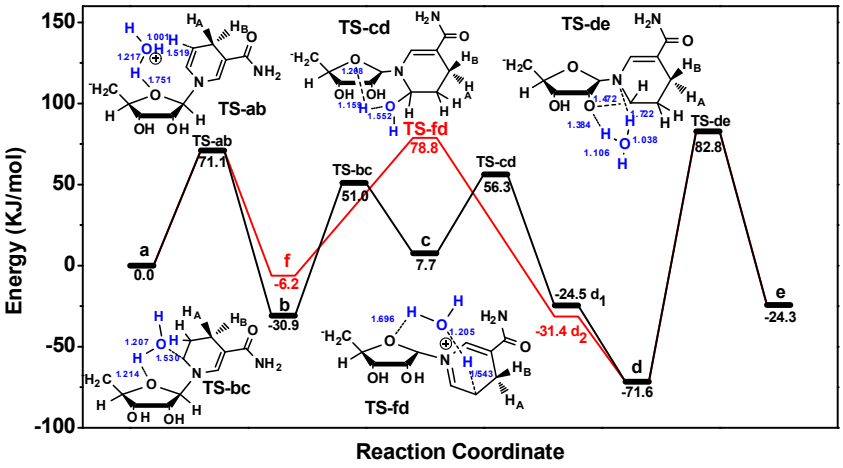

Figure 4. Calculated reaction pathways and energy profiles of the NADH model compound catalyzed by H_3O^+ at the B3LYP/6-311+g(d,p) level. The black and red curves denote two kinds of possible reaction pathways.

2.4. Enzymatic Reaction in BmimBF$_4$ and BmimDCA

2.4.1. Effect of NADH Degradation in BmimBF$_4$ and BmimDCA

pH was found to be the most crucial factor leading to NADH degradation. However, variation of pH value cannot be avoided given the intrinsic nature of the reaction. For instance, both the absorption of CO_2 into the aqueous solution and the formation of formic acid will result in a more acidic environment [33]. Interestingly, the results indicated that with CO_2, NADH degradation is significantly prevented in the presence of contained-BmimBF$_4$ buffer (Table 1, method **N**). To clarify and rationally understand this phenomenon, the influence of CO_2 absorption with and without BmimBF$_4$ on NADH degradation and pH variation were evaluated and compared. Experiments of NADH degradation were conducted in an aqueous solution with a range of volume ratio of BmimBF$_4$ to buffer in the presence or absence of CO_2 (Figure 5A). The degradation concentration-course plot (in black) in the case of without CO_2 offers a downward parabola. It demonstrated that the maximum degradation of NADH in a combination of BmimBF$_4$ and buffer is 22% when a volume ratio of 40% (V_{IL}/V_{buffer}) is reached. The in-situ pH evaluation of the solution (Figure 5B) indicated this degradation follows a function of pH value variation, with maximum degradation appearing at the lowest pH value. The pH value variation was attributed to the hydrolysis of BmimBF$_4$, which may occur with a different extent under these conditions [34]. On the other hand, a significant degradation of NADH was detected in the buffer as soon as CO_2 (1 bar) was introduced (Figure 5A, plot in red). Interestingly, such a degradation was gradually relieved with loading BmimBF$_4$ from 0 to 20% (V_{IL}/V_{buffer}). The stabilization has been attributed to the formation of ternary aggregates (CO_2/IL/H_2O), wherein the amphipathic BmimBF$_4$ could self-assemble at the interface between the nonpolar CO_2 and the aqueous phase [35]. In this manner, formation of carbonic acid was therefore avoided. Specifically, both hydrolysis of BmimBF$_4$ and the formation of carbonic acid will be inhibited when a higher ratio of V_{IL}/V_{buffer} was launched, with less NADH degradation.

In contrast, NADH is much more stable in the presence of a weakly basic BmimDCA (Figure 6A, plot in black), with less than 10% degradation of NADH occurring at maximum. The pH value of the solution progressively increased when the ratio of BmimDCA was increased (Figure 6B). A similar stabilization of NADH with IL functioning as the surface-active molecule was also observed when CO_2 was introduced (Figure 6A, plot in red).

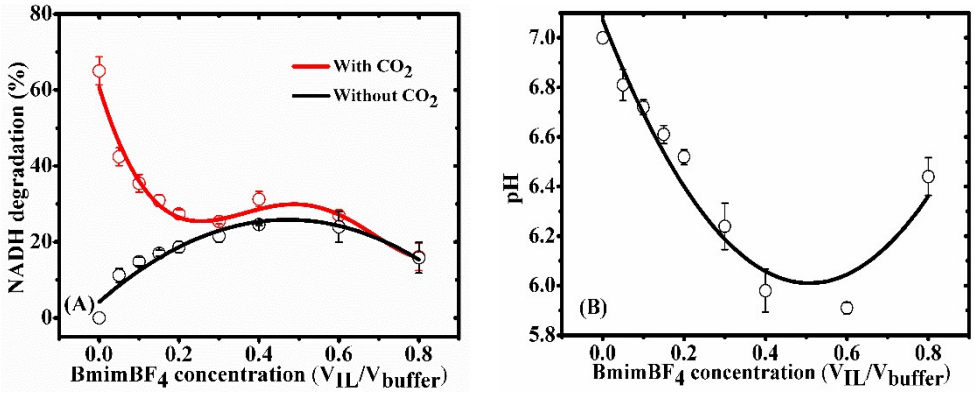

Figure 5. Effect of CO_2 on the degradation of NADH in $BmimBF_4$. (**A**) Degradation of NADH with CO_2 and without CO_2; (**B**) pH of solution at different concentrations of $BmimBF_4$; General conditions: NADH in contained-$BmimBF_4$ buffer for 3 h at 37 °C; NADH (1.4 mg, 2 μmol); CO_2 (1 bar); Buffer (2 mL).

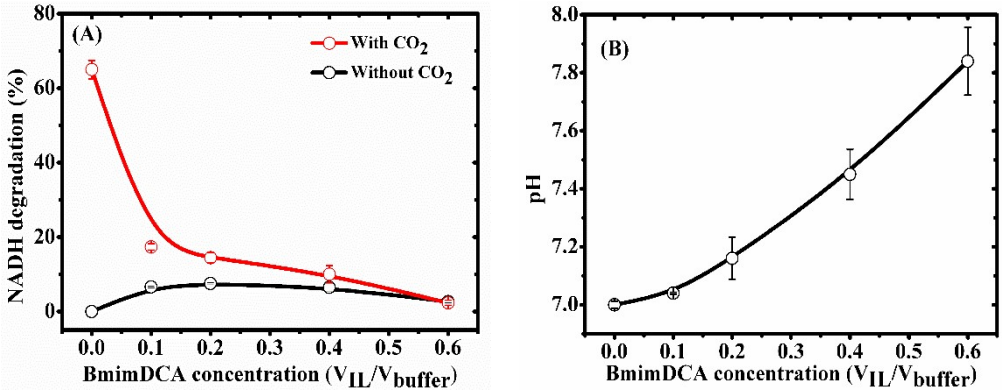

Figure 6. Effect of CO_2 on degradation of NADH in BmimDCA. (**A**) Degradation of NADH with CO_2 and without CO_2; (**B**) pH of solution at different concentrations of BmimDCA; General conditions: NADH in contained-BmimDCA buffer for 3 h at 37 °C; NADH (1.4 mg, 2 μmol); CO_2 (1 bar); Buffer (2 mL).

2.4.2. Enzymatic Reaction in $BmimBF_4$ and BmimDCA

Enzymatic conversion of CO_2 to formate in phosphate buffer systems (IL/buffer) consisting of two alternative ILs at different ratios was subsequently conducted (Table 3). As indicated by experiments of NADH degradation (Figure 5A), it will lead to not only the formation of a ternary aggregates (CO_2/IL/H_2O) but also hydrolysis of $BmimBF_4$ when the concentration of $BmimBF_4$ was increased within a range (V_{IL}/V_{buffer} < 50%), which actually has an opposite effect towards the degradation of NADH. Therefore, taking these premises into consideration, to find a proper concentration of $BmimBF_4$ is required to attain an optimized conversion with least NADH being degraded (entry 3). In contrast to the acidic $BmimBF_4$, NADH was more stable in the presence of basic BmimDCA. And the conversion of NADH monotonously decreased when the concentration of BmimDCA was increased (entries 6~9), but the yield of formate increased with the concentration of BmimDCA from 10% to 40%, and dropped to the lowest at 60% BmimDCA.

It is well known that water with small amounts of salts is considered to be the best media for proteins. However, high concentration of ILs (salts) can cause conformational changes of peptide chains that can result in enzyme denaturation [36]. Crystallisation and aggregation behaviour of proteins change dramatically upon increasing concentrations of ILs. Indeed, in pure ILs, enzymes can hardly be dissolved in homogenous phase without denaturation. In this enzymatic reaction, increasing concentration of IL to absorb CO_2 is expected to influence negatively the activity of the enzyme. This can explain that CO_2 conversion achieved the highest value when only a 20% of $BmimBF_4$ was used.

Table 3. Enzymatic Conversion of CO_2 to Formate [a].

Entry	Solvent (*v*/*v*)	NADH Conv. (%) (SD)	Yield of Formate (%) (SD)	pH (SD)	
		Method N	Method C	Before	After
1	Phosphate buffer	64.6 (±3.6)	1.1 (±0.5)	7.0 (±0.04)	5.6 (±0.08)
2	10% $BmimBF_4$	46.8 (±2.3)	0.2 (±0.3)	6.7 (±0.08)	6.2 (±0.12)
3	20% $BmimBF_4$	25.4 (±3.2)	2.9 (±0.4)	6.5 (±0.06)	6.0 (±0.16)
4	40% $BmimBF_4$	36.3 (±2.0)	2.3 (±0.4)	6.0 (±0.05)	5.8 (±0.18)
5	60% $BmimBF_4$	24.6 (±3.0)	0.6 (±0.3)	5.9 (±0.05)	5.6 (±0.19)
6	10% BmimDCA	34.0 (±3.9)	0.4 (±0.2)	7.0 (±0.04)	6.6 (±0.12)
7	20% BmimDCA	16.2 (±1.3)	1.5 (±0.5)	7.2 (±0.06)	6.5 (±0.14)
8	40% BmimDCA	4.9 (±2.8)	1.8 (±0.5)	7.5 (±0.08)	6.5 (±0.19)
9	60% BmimDCA	1.6 (±1.4)	0.2 (±0.2)	7.8 (±0.09)	6.8 (±0.20)

[a] Reaction conditions: FDH (3 µL, 0.075 U/mL), NADH (2 µmol, 1 mM), CO_2 (1 bar), buffer (100 mM (Na_2HPO_4:NaH_2PO_4 = 39:61 (mol/mol)), 2 mL); 37 °C, 3 h. [a] Enzymatic reaction was repeated three times and standard deviations (SD) were calculated that presented in the Table 3. pH value of reaction mixture was added before and after saturating CO_2.

2.4.3. Multi-Enzymatic Reaction of Converting CO_2 to Methanol in $BmimBF_4$

Sequential reduction of CO_2 to formic acid, formaldehyde and finally methanol is limited by the low reaction rate of the first reaction in the sequence (CO_2 → formic acid), which is much lower than that of the reverse reaction (formic acid → CO_2) [9]. Indeed formic acid oxidation was 30 times faster than CO_2 reduction catalyzed by FDH [29]. For the second enzyme, FaldDH, the reaction (formic acid → formaldehyde) was also found to be less efficient than the reverse reaction (formaldehyde → formic acid). However, for the third enzyme, ADH, the forward reaction (formaldehyde → methanol) is much more favorable than the reverse reaction (methanol → formaldehyde). Therefore, to make this multi-enzymatic reaction efficient, formic acid and formaldehyde have to be consumed by the next sequential reaction, in order to shift the equilibrium of the cascade reaction and eventually achieving high conversion of CO_2 to methanol (Table 4, entry 1).

Table 4. Enzymatic Conversion of CO_2 to Methanol [b].

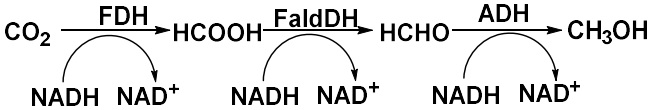

Entry	Solvent (v_{IL}/v_{buffer})	Yield of Methanol (%) (SD)
1	Phosphate buffer	24.3 (±1.2)
2	$BmimBF_4$ (10%)	20.2 (±1.9)
3	$BmimBF_4$ (20%)	67.1 (±2.4)
4	$BmimBF_4$ (40%)	48.3 (±2.1)
5	$BmimBF_4$ (60%)	15.2 (±2.6)

[b] Reaction conditions: FDH (3 µL, 0.075 U/mL), FalDH (0.2 mg, 0.1 U/mL), ADH (0.2 mg, 30 U/mL), NADH (2 µmol, 1 mM), CO_2 (1 bar), buffer (100 mM phosphate, pH = 7); 37 °C, 3 h. Standard deviation (SD).

Another strategy to further increase conversion of CO_2 to methanol is to enhance CO_2 solubility, as low CO_2 solubility in water would also result in low formic acid concentration. As a consequence, production of formaldehyde is prevented, as the second sequential reaction requires a threshold concentration of formic acid to be activated [24]. Both factors (unfavourable equilibrium rates and need of a minimum concentration threshold) make the first reaction of the sequence (the one studied here) to play a decisive role on conversion of CO_2 to methanol. Addition of $BmimBF_4$ helps enhance the conversion in the first reaction by both stabilizing NADH and also increasing CO_2 solubility. Indeed, the yield of methanol when the reaction was conducted in 20% $BmimBF_4$ was two times higher than in the phosphate buffer.

Other authors followed other strategies to increase conversion. For example, Ober and Dave immobilized the three enzymes in silica sol-gel matrixes, confining and reducing the volume of the

enzymes, in such a manner that the local concentration of reactants was enhanced [8]. Jiang followed a similar strategy, and was able to increase the yield of methanol up to 71.6% [24]. These studies also confirmed that breaking the unfavourable equilibrium by switching it to the right is a good manner to enhance the overall conversion.

3. Materials and Methods

3.1. Materials

Formate dehydrogenase (EC 1.2.1.2, homo-dimer, 76 kDa) from *Candida boidinii* (FDH), formaldehyde dehydrogenase (EC 1.2.1.46, homo-dimer, 150 kDa) from *Pseudomonas* sp. (FaldDH), alcohol dehydrogenase (EC 1.1.1.1, homo-tetramer, 141 kDa) from Saccharomyces cerevisiae (ADH), β-Nicotinamide adenine dinucleotide reduced form (NADH, >97 wt %), and β-Nicotinamide adenine dinucleotide hydrate (NAD^+, >98 wt %) were purchased from Sigma Aldrich. Formate, sodium phosphates, citric acid, acetamide, isopropanol, sodium acetate, and acetic anhydride and were supplied by Sinopharm chemical agent (Shanghai, China). CO_2 gas (>99.99%) in a cylinder was supplied by Beijing Beiwen Gas Factory. 1-butyl-3-methylimidazolium tetrafluoroborate ($BmimBF_4$), 1-ethyl-3-methylimidazolium tetrafluoroborate ($EmimBF_4$), 1-ethyl-3-methylimidazolium acetate (EmimOAc), 1-butyl-3-methylimidazolium dicyanamide (BmimDCA), and 1-butyl-3-methylimidazolium dimethylphosphate (BmimDMP) (purity > 99.0 wt %) were purchased from Lanzhou Institute of Chemical Physics (Lanzhou, China). 1,8-Diazabicyclo[5.4.0]undec-7-ene lactate (DBULat) (purity > 98.0 wt %) were purchased from Linzhou Keneng material technology corporation. Ultra-pure water was obtained using a water purification system (Milli-Q Direct 8).

3.2. General Procedure for Enzymatic Conversion of CO_2 to Formate

The enzymatic reaction was conducted in a stainless steel reactor (25 mL) equipped with two valves and a pressure gauge. In the reactor, a buffer solution of FDH (3 μL) and NADH (1 mM) was bubbled with CO_2 for 5 min to remove the residual air, after which the pressure was adjusted to 1 bar. The reactor was positioned in water bath at 37 °C for 3 h. Samples were then taken from the reactor for analysis. Buffer (100 mM (Na_2HPO_4:NaH_2PO_4 = 39:61 (mol/mol)), pH = 7, 2 mL); Enzymatic reaction was repeated three times; standard deviations (SD) were calculated and presented in the Table 1.

3.3. Kinetic Degradation of NADH in $BmimBF_4$

Solution of NADH and $BmimBF_4$ was prepared in deionized water (2 mL) at concentration of 1 mM (1.4 mg, 2 μmol) and 5 mM (2 μL, 5.0 equiv.), respectively. The reaction was performed over a temperature range of 10–80 °C during which sample was measured every ten degree centigrade and kept for ten minutes. Additionally, another experiment was carried out at 37 °C for 9 h and the preparation of sample was same as above during which samples were measured every ten minutes (Figure 1B). Temperature (37 °C) in such experiment was referring to enzymatic reaction and the variation of NADH concentration with time was monitored by method **N**.

3.4. Stability of NADH in Aqueous ILs

In the reactor, a solution (2 mL) of 20 vol % ILs and 80 vol % deionized water was prepared to dissolve 2 μmol NADH (1 mM). Then, the reactor was positioned in water bath at 37 °C for 3 h. The sample was taken from the reactor and detected at 340 nm by an in-situ UV–vis spectroscopy (Table 2).

3.5. Effect of Acidity on the Degradation of NADH

Phosphate buffers in the pH range of 1.0–7.0 were separately prepared, namely, pH 7, 6.5, 5.0, 4.5, 4.0, 3.5, 3.0, 2.5, 2.0, 1.5, and 1.0, with addition of varied amounts of purity phosphoric acid in

phosphate solution (pH = 7). NADH (1 mM) in these buffers was separately incubated at 37 °C for 3 h. Residue NADH is measured at 340 nm by an in-situ UV–vis spectroscopy (Figures 2 and S6).

3.6. NMR for NADH Degradation in $BmimBF_4$

Equimolar of NADH and $BmimBF_4$ was mixed in deuteroxide. The mixture was heated at 50 °C for 3 h and then the product was purified through extraction of methylene dichloride. After removing methylene dichloride in a vacuum oven at 50 °C for 3 h, solid powder was obtained and detected by NMR.

3.7. Effect of NADH Degradation in $BmimBF_4$ and BmimDCA

Solutions (2 mL) of $BmimBF_4$ with phosphate buffer in different concentration were prepared, namely, 0%, 5%, 10%, 15%, 20%, 30%, 40%, 60%, and 80% (V_{IL}/V_{buffer}). In the reactor, NADH (1 mM) in the prepared solution was bubbled with CO_2 for 5 min to remove the residual air, after which the pressure was adjusted to 1 bar. The reactor was positioned in water bath at 37 °C for 3 h. Without CO_2, it is no need to press CO_2 in the reactor. In the same way, solutions (2 mL) of BmimDCA with phosphate buffer in different concentrations were prepared, namely, 0%, 10%, 20%, 30%, 40%, and 60% (V_{IL}/V_{buffer}). In the reactor, NADH (1 mM) in the solution was bubbled with CO_2 for 5 min to remove the residual air, after which the pressure was adjusted to 1 bar. The reactor was positioned in water bath at 37 °C for 3 h. Furthermore, pH value of each solution was measured by pH meter (298.5 K, Mettler Toledo FE20, Mettler Toledo, Zurich, Zurich State, Switzerland) before starting reaction.

3.8. Enzymatic Reaction in $BmimBF_4$ and BmimDCA

Solutions (2 mL) of $BmimBF_4$ with phosphate buffer in different concentrations were prepared, namely, 0%, 10%, 40%, and 60% (V_{IL}/V_{buffer}). Solutions (2 mL) of $BmimBF_4$ with phosphate buffer were prepared in the same way. Procedure of enzymatic reaction is as same as described above (General procedure).

3.9. Analytical Method

Two methods, NADH (named as **N**) and colorimetric detection (named as **C**), were evaluated to determine the yield of formate product. The details of these methods are as follows:

*3.10. Method **N** for Determination Concentration of NADH*

Method **N** is an indirect method where the yield of formate is determined through quantifying reduction of NADH. It can be easily monitored by UV–vis spectroscopy at 340 nm referenced to NADH [23]. The assumption is that formation of formate during the enzyme-catalysed process would consume an equal-molar amount of NADH. The concentration of NADH was quantified by absorbance measurements, which was monitored at 340 nm by an in-situ UV–vis spectroscopy. After the enzymatic conversion to formate was completed, 0.5 mL of sample was taken and diluted with 1.5 mL of water. After dilution of NADH solution, absorbance at 340 nm is below 2 that is more precise. Then 2 mL of the solution was pipetted into a 10 mm quartz cell. The photometric measurement was monitored at 340 nm using a UV–vis spectrophotometer (Shimadzu UV, 2550 spectrophotometer Shimadzu Corporation, Tokyo, Tokyo metropolitan, Japan). The standard calibration curve is presented in Figure S1.

3.11. Method C for Determination Concentration of Formate

Method **C** was originally used for detecting formate in products from fermentation [37]. The assumption is that a complex compound, recorded at 515 nm using UV–vis spectroscopy, would be formed by the reaction of formate with a mixture of citric acid, isopropanol, acetic anhydride, sodium acetate in an appropriate ratio [38]. The yield of formate is then directly determined. First, 3.5 mL of 100% acetic anhydride, 50 µL of 30% (*w*/*v*) sodium acetate, and 1 mL of 2-propanol solution

containing 0.5% (*w*/*v*) citric acid and 10% (*w*/*v*) acetamide were added in a 10 mL vial. Then 0.5 mL of sample was added to this assay solution and incubated for 90 min at 25 °C. Finally, the absorbance was determined at 515 nm using a UV–vis spectrophotometer. The formate standard calibration curve was prepared against the appropriate concentrations of formate (Figures S2–S4). 500 µL of sample was used for the colorimetric assay.

3.12. GC for Determination Concentration of Methanol

A Hewlett Packard HP6890 gas chromatograph (Hewlett-Packard Company, Palo Alto, CA, USA) (GC) equipped with a FID (250 °C) and a Restek XTI-5 column (30 m × 0.25 mm i.d., film thickness 0.25 mm) was used for methanol concentration by using ethyl acetate as an internal standard. The carrier gas was N_2 with a flow rate of 0.4 mL min^{-1}. The injector temperature was 150 °C and the injection volume was 1 mL. Methanol GC chromatograms were calibrated with 0.01–1 mM methanol solution in 0.1 M pH 7.0 phosphate buffer.

3.13. ^1H Nuclear Magnetic Resonance Measurements

Spectra were recorded at 298 K on a Bruker av-600 MHz spectrometer (Bruker, Bilka, MA, USA) operating at 600 MHz. Deuterium oxide was as solvent.

4. Conclusions

In summary, we demonstrated that NADH degradation is unavoidable due to the presence of acid gas during enzymatic CO_2 conversion, which impedes the CO_2 conversion and overestimates the conversion when the absorbance of NADH is used as a method of detection. The mechanism of NADH degradation was investigated by UV, NMR, and DFT calculation and all methods suggested that the occurrence of acid in the reaction mixture is the main contributing factor to the degradation observed. By selecting neutral–basic ionic liquids and adjusting the concentration of ionic liquids in the buffer, stabilization of the cofactor (NADH) can be achieved, along with enabling a higher CO_2 concentration in the buffer. Finally, CO_2 conversion was more than twice as compared with the conversion reached by the enzymatic reaction in a phosphate buffer (traditional buffer). This study is a significant contribution to the use of enzymes like formate dehydrogenase in ionic liquids and paves the way for improving biocatalysts using ionic liquids.

Supplementary Materials: The following are available online at http://www.mdpi.com/2073-4344/8/8/304/s1, **Figure S1**. Standard calibration curve for NADH method. **Figure S2**. Standard calibration of formate for colorimetric method in buffer. **Figure S3**. Standard calibration curve of formate for colorimetric method in BmimBF4. **Figure S4**. Standard calibration curve of formate for colorimetric method in BmimDCA. **Figure S5**. Arrhenius plots for degradation of NADH in BmimBF4 as temperature increases. **Figure S6**. NADH degrades in phosphate buffer whose pH in range from 7.0 to 4.5. **Figure S7**. NADH degrades in contained-BmimBF4 reaction. **Figure S8**. NADH degrades in ILs. **Figure S9**. Two possible pathway (red and black) for NADH degradation mechanism proposed by the Norman and co-worker. **Figure S10.** 1H NMR (600 MHz, D2O, 298K) (δ: ppm). (a) BmimBF4; (b) NADH; (c), NAD+; (d) a mixture of NADH and BmimBF4 (molar ratio = 1:1); D2O was used as the solvent. **Table S1** Structure for the NADH and its derivatives. **Table S2**. Summary of chemicals NMR data.

Author Contributions: Z.Z., B.-h.X. and J.L. conceived and designed the experiment, performed the experiments, and analysed the data. M.P., N.V.S. and S.Z. wrote the paper and reviewed drafts of the paper. H.H. and Y.Z. conceived and designed the simulation experiment, analysed the data and reviewed drafts of the paper.

Acknowledgments: The authors are thankful for support from National Science Foundation of China (U1704251) and (U1662133), CAS 100-Talent Program (2014).

Conflicts of Interest: The authors declare no conflict of interest.

References

1. Shi, J.F.; Jiang, Y.J.; Jiang, Z.Y.; Wang, X.Y.; Wang, X.L.; Zhang, S.H.; Han, P.P.; Yang, C. Enzymatic conversion of carbon dioxide. *Chem. Soc. Rev.* **2015**, *44*, 5981–6000. [CrossRef] [PubMed]

2. He, M.Y.; Sun, Y.H.; Han, B.X. Green carbon science: Scientific basis for integrating carbon resource processing, utilization, and recycling. *Angew. Chem. Int. Ed.* **2013**, *52*, 9620–9633. [CrossRef] [PubMed]
3. Xu, B.H.; Wang, J.Q.; Sun, J.; Huang, Y.; Zhang, J.P.; Zhang, X.P.; Zhang, S.J. Fixation of CO_2 into cyclic carbonates catalyzed by ionic liquids: A multi-scale approach. *Green Chem.* **2015**, *17*, 108–122. [CrossRef]
4. Cui, G.K.; Wang, J.J.; Zhang, S.J. Active chemisorption sites in functionalized ionic liquids for carbon capture. *Chem. Soc. Rev.* **2016**, *45*, 4307–4339. [CrossRef] [PubMed]
5. Hao, L.D.; Zhao, Y.F.; Yu, B.; Yang, Z.Z.; Zhang, H.Y.; Han, B.X.; Gao, X.; Liu, Z.M. Imidazolium-based ionic liquids catalyzed formylation of amines using carbon dioxide and phenylsilane at room temperature. *ACS Catal.* **2015**, *5*, 4989–4993. [CrossRef]
6. Dominguez-Benetton, X.S.S.; Satyawali, Y.; Vanbroekhoven, K.; Pant, D. Enzymatic electrosynthesis: An overview on the progress in enzyme-electrodes for the production of electricity, fuels and chemicals. *J. Microb. Biochem. Technol.* **2013**, *S6*, 007.
7. Srikanth, S.G.Y.A.; Vanbroekhoven, K.; Pant, D. Enzymatic electrosynthesis of formic acid through carbon dioxide reduction in a bioelectrochemical system: Effect of immobilization and carbonic anhydrase addition. *ChemPhysChem* **2017**, *18*, 3174–3181. [CrossRef] [PubMed]
8. Obert, R.; Dave, B.C. Enzymatic conversion of carbon dioxide to methanol: Enhanced methanol production in silica sol-gel matrices. *J. Am. Chem. Soc.* **1999**, *121*, 12192–12193. [CrossRef]
9. Luo, J.Q.; Meyer, A.S.; Mateiu, R.V.; Pinelo, M. Cascade catalysis in membranes with enzyme immobilization for multi-enzymatic conversion of CO_2 to methanol. *New Biotechnol.* **2015**, *32*, 319–327. [CrossRef] [PubMed]
10. Zhang, X.P.; Zhang, X.C.; Dong, H.F.; Zhao, Z.J.; Zhang, S.J.; Huang, Y. Carbon capture with ionic liquids: Overview and progress. *Energy Environ. Sci.* **2012**, *5*, 6668–6681. [CrossRef]
11. D'Alessandro, D.M.; Smit, B.; Long, J.R. Carbon dioxide capture: Prospects for new materials. *Angew. Chem. Int. Ed.* **2010**, *49*, 6058–6082. [CrossRef] [PubMed]
12. Kenarsari, S.D.; Yang, D.L.; Jiang, G.D.; Zhang, S.J.; Wang, J.J.; Russell, A.G.; Wei, Q.; Fan, M.H. Review of recent advances in carbon dioxide separation and capture. *RSC Adv.* **2013**, *3*, 22739–22773. [CrossRef]
13. Zhao, Z.J.; Dong, H.F.; Zhang, X.P. The research progress of CO_2 capture with ionic liquids. *Chin. J. Chem. Eng.* **2012**, *20*, 120–129. [CrossRef]
14. Blanchard, L.A.; Gu, Z.Y.; Brennecke, J.F. High-pressure phase behavior of ionic liquid/CO_2 systems. *J. Phys. Chem. B* **2001**, *105*, 2437–2444. [CrossRef]
15. Lau, R.M.; van Rantwijk, F.; Seddon, K.R.; Sheldon, R.A. Lipase-catalyzed reactions in ionic liquids. *Org. Lett.* **2000**, *2*, 4189–4191.
16. Datta, S.; Holmes, B.; Park, J.I.; Chen, Z.W.; Dibble, D.C.; Hadi, M.; Blanch, H.W.; Simmons, B.A.; Sapra, R. Ionic liquid tolerant hyperthermophilic cellulases for biomass pretreatment and hydrolysis. *Green Chem.* **2010**, *12*, 338–345. [CrossRef]
17. Eckstein, M.; Villela, M.; Liese, A.; Kragl, U. Use of an ionic liquid in a two-phase system to improve an alcohol dehydrogenase catalysed reduction. *Chem. Commun.* **2004**, 1084–1085. [CrossRef] [PubMed]
18. Zhao, R.H.; Zhang, X.W.; Zheng, L.; Xu, H.; Li, M. Enantioselective esterification of (*R*,*S*)-flurbiprofen catalyzed by lipase in ionic liquid. *Green Chem. Lett. Rev.* **2017**, *10*, 23–28. [CrossRef]
19. Zhu, C.H.; Guo, F.; Guo, X.Q.; Li, X.K. In situ saccharification of cellulose using a cellulase mixture and supplemental beta-glucosidase in aqueous-ionic liquid media. *Bioresources* **2016**, *11*, 9068–9078. [CrossRef]
20. Amado, V.C.F. *"One-Pot" Enzymatic Conversion of CO_2 to Methanol*; Faculdade de Ciências e Tecnologia: Caparica, Portugal, 2013.
21. Kaftzik, N.; Wasserscheid, P.; Kragl, U. Use of ionic liquids to increase the yield and enzyme stability in the beta-galactosidase catalysed synthesis of *N*-acetyllactosamine. *Org. Process Res. Dev.* **2002**, *6*, 553–557. [CrossRef]
22. Dabirmanesh, B.; Khajeh, K.; Ranjbar, B.; Ghazi, F.; Heydari, A. Inhibition mediated stabilization effect of imidazolium based ionic liquids on alcohol dehydrogenase. *J. Mol. Liq.* **2012**, *170*, 66–71. [CrossRef]
23. Lu, Y.; Jiang, Z.Y.; Xu, S.W.; Wu, H. Efficient conversion of CO_2 to formic acid by formate dehydrogenase immobilized in a novel alginate-silica hybrid gel. *Catal. Today* **2006**, *115*, 263–268. [CrossRef]
24. Wang, X.; Li, Z.; Shi, J.; Wu, H.; Jiang, Z.; Zhang, W.; Song, X.; Ai, Q. Bioinspired approach to multienzyme cascade system construction for efficient carbon dioxide reduction. *ACS Catal.* **2014**, *4*, 962–972. [CrossRef]
25. Liu, A.H.; Feng, R.R.; Liang, B. Microbial surface displaying formate dehydrogenase and its application in optical detection of formate. *Enzyme Microb. Technol.* **2016**, *91*, 59–65. [CrossRef] [PubMed]

26. Anderson, A.G.; Berkelhammer, G. A study of the primary acid reaction on model compounds of reduced diphosphopyridine nucleotide. *J. Am. Chem. Soc.* **1958**, *80*, 992–999. [CrossRef]
27. Alivisatos, S.G.; Ungar, F.; Abraham, G.J. Spontaneous reactions of 1,3-substituted 1,4-dihydropyridines with acids in water at neutrality.I. Kinetic analysis and mechanism of reactions of dihydronicotinamide—adenine dinucleotide with orthophosphates. *Biochemistry* **1965**, *4*, 2616–2630.
28. Oppenheimer, N.J.; Kaplan, N.O. Structure of the primary acid rearrangement product of reduced nicotinamide adenine dinucleotide (NADH). *Biochemistry* **1974**, *13*, 4675–4685. [CrossRef] [PubMed]
29. Ruschig, U.; Muller, U.; Willnow, P.; Hopner, T. CO_2 reduction to formate by nadh catalyzed by formate dehydrogenase from pseudomonas-oxalaticus. *Eur. J. Biochem.* **1976**, *70*, 325–330. [CrossRef] [PubMed]
30. Wang, Y.Z.; Li, M.F.; Zhao, Z.P.; Liu, W.F. Effect of carbonic anhydrase on enzymatic conversion of CO_2 to formic acid and optimization of reaction conditions. *J. Mol. Catal. B-Enzym.* **2015**, *116*, 89–94. [CrossRef]
31. Rover, L.; Fernandes, J.C.B.; Neto, G.D.; Kubota, L.T.; Katekawa, E.; Serrano, S.H.P. Study of nadh stability using ultraviolet-visible spectrophotometric analysis and factorial design. *Anal. Biochem.* **1998**, *260*, 50–55. [CrossRef]
32. Frisch, M.J.T.G.W.; Schlegel, H.B.; Scuseria, G.E.; Robb, M.A.; Cheeseman, J.R.; Scalmani, G.; Barone, V.; Mennucci, B.; Petersson, G.A.; Nakatsuji, H.; et al. *Gaussian 09, Revision d. 01*; Gaussian, Inc.: Wallingford, CT, USA, 2013.
33. Baltrusaitis, J.; Grassian, V.H. Carbonic acid formation from reaction of carbon dioxide and water coordinated to al(oh)(3): A quantum chemical study. *J. Phys. Chem. A* **2010**, *114*, 2350–2356. [CrossRef] [PubMed]
34. Freire, M.G.; Neves, C.M.S.S.; Marrucho, I.M.; Coutinho, J.A.P.; Fernandes, A.M. Hydrolysis of tetrafluoroborate and hexafluorophosphate counter ions in imidazolium-based ionic liquids. *J. Phys. Chem. A* **2010**, *114*, 3744–3749. [CrossRef] [PubMed]
35. Carrete, J.; Mendez-Morales, T.; Cabeza, O.; Lynden-Bell, R.M.; Gallego, L.J.; Varela, M.L. Investigation of the local structure of mixtures of an ionic liquid with polar molecular species through molecular dynamics: Cluster formation and angular distributions. *J. Phys. Chem. B* **2012**, *116*, 5941–5950. [CrossRef] [PubMed]
36. Yuki Kohno, H.O. Ionic liquid/water mixtures: From hostility to conciliation. *Chem. Commun.* **2012**, *48*, 7119–7130. [CrossRef] [PubMed]
37. Sleat, R.; Mah, R.A. Quantitative method for colorimetric determination of formate in fermentation media. *Appl. Environ. Microb.* **1984**, *47*, 884–885.
38. Denning, D.M.; Thum, M.D.; Falvey, D.E. Photochemical reduction of CO_2 using 1,3-dimethylimidazolylidene. *Org. Lett.* **2015**, *17*, 4152–4155. [CrossRef] [PubMed]